Conformational Stability from Rare Gas Solutions, r_0 Structural Parameters, Barriers to Internal Rotation, and Ab initio Calculations for Vinyl Silyl Fluoride

Yasser E. Nashed,[†,‡] Mohammad A. Qtaitat,[§] Chao Zheng,[†] Xiaohua Zhou,[†] Gamil A. Guirgis,[||] Joann F. Sullivan,[⊥] and James R. Durig*[,†]

Department of Chemistry, University of Missouri-Kansas City, Kansas City, Missouri 64110, Department of Chemistry, Mu'tah University, Karak, Jordan, Department of Chemistry and Biochemistry, College of Charleston, South Carolina 29424, Medical University of South Carolina, Charleston, South Carolina 29425

Received: August 24, 2008; Revised Manuscript Received: November 14, 2008

The Raman (3300−10 cm^{-1}) and infrared (3300−40 cm^{-1}) spectra of gaseous and solid vinyl silyl fluoride, CH_2═$CHSiH_2F$, have been recorded. Raman spectrum of the liquid has also been recorded and depolarization values obtained. Variable-temperature studies of the infrared spectra of the sample dissolved in liquid krypton (−110 to −150 °C) and liquid xenon (−60 to −100 °C) have been carried out. From these studies, the enthalpy difference has been determined to be 76 ± 7 cm^{-1} (0.91 ± 0.08 kJ/mol) from the krypton solutions and 69 ± 7 cm^{-1} (0.82 ± 0.08 kJ/mol) from the xenon solutions, with the gauche conformer the more stable form. From the far-infrared spectrum of the gas, the asymmetric torsional fundamentals for the cis and gauche conformers have been observed at 102.34 and 86.56 cm^{-1}, respectively, with each having several "hot bands" falling to lower frequencies. From these frequencies along with the experimentally determined conformational enthalpy difference, as well as the gauche skeletal dihedral angle, the potential function governing the conformational interchange has been determined with the following Fourier cosine potential coefficients: V_1 = −80 ± 11, V_2 = −42 ± 15, V_3 = 622 ± 5, V_4 = 34 ± 5, and V_6 = −31 ± 2 cm^{-1}. The gauche-to-cis and gauche-to-gauche barriers are 664 cm^{-1} (7.94 kJ/mol) and 608 cm^{-1} (7.27 kJ/mol), respectively. Complete vibrational assignments are provided for both conformers. In addition, equilibrium geometries and electronic energies have been determined for both rotamers from ab initio calculations using restricted Hartree−Fock and Møller−Plesset perturbation method to the second order (MP2), as well as density functional theory by the B3LYP methods, employing a number of basis sets up to 6−311+G(2df,2pd). All levels of calculation predict the gauche conformer to be the more stable form. By systematically adjusting the ab initio predicted structural values to fit the previously reported microwave rotational constants, adjusted r_0 parameters have been obtained for both conformers. These values are compared to those for the corresponding chloride and methyl compounds. The spectroscopic and theoretical results are discussed and compared to the corresponding quantities for some similar molecules.

Introduction

In the past decade, we have measured the conformational stability of a series of allyl halides (3-halopropenes), CH_2═$CHCH_2X$ where X = F,[1] Cl,[2] Br[3] and I.[4] Allyl fluoride has the cis conformer as the more stable form, whereas all of the other allyl halides have the gauche conformer more stable. We have also carried out ab initio calculations for the fluoride and chloride utilizing several basis sets by the Møller−Plesset perturbation theory[5] to the second order. However, from ab initio MP2/6−311++G(d,p) calculations for the fluoride,[6] the gauche conformer is predicted to be the lower-energy form by 117 cm^{-1} (1.40 kJ/mol), which is at variance with the experimental results with a determined enthalpy difference of 81 ± 1 cm^{-1} (0.97 ± 0.01 kJ/mol) from a liquid argon solution and 130 ± 25 cm^{-1} (1.56 ± 0.30 kJ/mol) from the vapor,[1] with the cis conformer the more stable form. For the corresponding chloride, ab initio MP2/6−311++G(d,p) calculations predict the gauche conformer more stable than the cis form by 457 cm^{-1} (5.47 kJ/mol), whereas the experimental value is 147 ± 20 cm^{-1} (1.76 ± 0.24 kJ/mol) from a variable temperature infrared study of liquid xenon solutions.[2] These limited results indicate that this level of calculation overestimates the gauche stability by 200−300 cm^{-1} for allyl halides, when diffuse functions are utilized. Even at the level of QCISD/6−311++G(d,p), ab initio calculations incorrectly predict the gauche conformer to be more stable by 50 cm^{-1} (0.60 kJ/mol) for 3-fluoropropene.[6]

As a continuation of our conformational and structural studies of allyl halides and their sila-analogues (CH_2═$CHSiH_2X$), we reported[7] the conformational stability and the vibrational spectra of vinyl silyl chloride (CH_2═$CHSiH_2Cl$) for which the most stable conformer has been identified to be the gauche form with an experimental enthalpy difference of 78 ± 11 cm^{-1} (0.93 ± 0.13 kJ/mol) in liquid xenon solution. The correct conformational stability is predicted from the MP2 calculations with basis sets 6−31G(d) to moderately sized basis set of MP2(full)/6−311+G(2d,2p) with an energy difference of 21 cm^{-1} (0.25 kJ/mol). Therefore, the ab initio predictions for vinyl silyl chloride did not over estimate the stability of the gauche conformer as found for the corresponding carbon molecule.

* Corresponding author. Phone: 01 816-235-6038. Fax: 01 816-235-2290. E-mail: durigj@umkc.edu..
[†] University of Missouri-Kansas City.
[‡] Current address: Department of Analytical Sciences, Amgen Inc., Thousand Oaks, CA 91320.
[§] Mu'tah University.
[||] College of Charleston.
[⊥] University of South Carolina.

10.1021/jp8076547 CCC: $40.75
Published on Web 01/30/2009

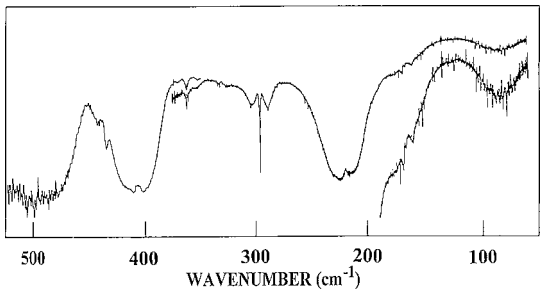

Figure 1. Far infrared spectrum of gaseous vinyl silyl fluoride.

Additionally, we were interested to learn whether ab initio calculations would correctly predict the more stable conformer for vinyl silyl fluoride and whether the more stable conformer would be the cis conformer as found for allyl fluoride. From an earlier microwave study[8] of vinyl silyl fluoride, the gauche conformer was reported to be more stable than the cis form by 210 ± 140 cm^{-1} (2.51 ± 1.68 kJ/mol). However, the value of enthalpy difference may be questionable because the uncertainty is very high and it is known that determination of conformer stabilities from microwave data is a formidable task. Additionally, utilizing the vibrational satellites in the microwave spectra, the asymmetric torsion and CSiF bending modes for the *gauche* conformer were estimated to be 74 ± 18 and 181 ± 39 cm^{-1}, respectively. Again, the uncertainties of these quantities are high and they are the only known reported vibrational frequencies for this molecule. Thus, we have investigated the vibrational spectra of this molecule in order to determine the conformational enthalpy difference from temperature dependent infrared spectra of rare gas solutions. We also investigated the far-infrared spectra to assign the fundamental and excited-state torsional modes for both conformers to obtain the potential function governing the barrier to internal rotation. For comparison with experimental results, we have carried out ab initio calculations utilizing a variety of basis sets up to 6−311+G(2df,2pd) at the levels of restricted Hartree−Fock and Møller−Plesset perturbation theory to the second order,[5] as well as hybrid density functional theory by the B3LYP method[9,10] to determine the conformational stability as well as the structural parameters for both the cis and gauche conformers of vinyl silyl fluoride. By systematically adjusting the ab initio equilibrium structural values to fit the previously reported microwave rotational constants,[8] adjusted r_0 structural parameters have been obtained for both conformers. The results of these spectroscopic and theoretical studies are reported herein with comparison to the corresponding carbon analogues.

Experimental Section

The sample of vinyl silyl fluoride was prepared by the fluorination of vinyl silyl chloride, $CH_2{=}CHSiH_2Cl$, which was accomplished by passing it over freshly sublimed antimony trifluoride at room temperature. Vinyl silyl chloride was prepared by the reaction of vinyl silane with silver chloride.[11] Preparation and sample handling was carried out under a vacuum to minimize sample contamination by air and water. The sample was purified by a low-temperature, low-pressure fractionation column.

The low-frequency infrared spectrum (Figure 1) of the gas was obtained with a Digilab model FTS-15B Fourier transform spectrometer equipped with a 6.25 μm Mylar beamsplitter and a DTGS detector. The spectrum was recorded with the sample contained in a 10-cm cell fitted with polyethylene windows.

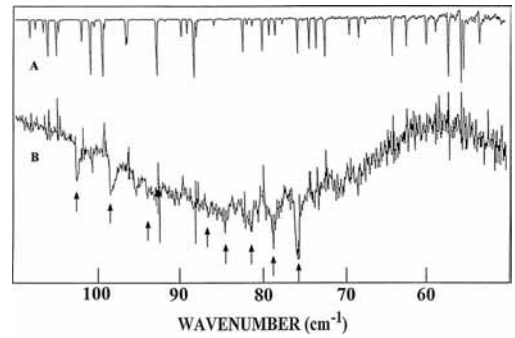

Figure 2. Far infrared spectra: (A) spectrum of water from background; (B) gaseous vinyl silyl fluoride in the region of asymmetric torsional mode, ↑ indicating transition listed inTable 6S.

The far-infrared spectrum from which the torsional transitions were obtained (Figure 2) was recorded on a Nicolet model 200 SXV Fourier-transform spectrometer equipped with a vacuum bench and a liquid helium cooled germanium bolometer containing a wedged sapphire filter and polyethylene window with a 6.25 μm Mylar beamsplitter. The sample was contained in a one meter cell fitted with polyethylene windows and interferograms were collected at an effective resolution of 0.10 cm^{-1}.

The mid-infrared spectra (3300 to 400 cm^{-1}) were recorded with a Digilab model FTS-14C Fourier transform spectrometer equipped with a Globar source, a Ge/KBr beamsplitter and a TGS detector. Atmospheric water vapor was removed from the spectrometer housing by purging with dry nitrogen. For the gas, the spectrum was recorded with the sample contained in a 12 cm cell equipped with CsI windows. Interferograms were obtained after 512 scans for both the sample and reference and transformed using a boxcar truncation function with a theoretical resolution of 0.5 cm^{-1}. The mid-infrared spectrum of the solid was obtained by depositing the sample on a CsI substrate held at about −196 °C by boiling liquid nitrogen. The substrate was housed in a low-temperature cold cell fitted with CsI windows. The sample was repeatedly annealed until no further changes were observed in the spectrum. The spectrum of the solid was obtained from 300 scans for both the sample and the reference with a resolution of 1 cm^{-1}.

The mid-infrared spectra of the samples dissolved in liquified krypton (Figure 3A) and xenon as a function of temperature were recorded on a Bruker model IFS-66 Fourier transform spectrometer equipped with a Globar source, a Ge/KBr beamsplitter and a DTGS detector. The temperature studies ranged from −110 to −150 °C for liquid krypton and −60 to −100 °C for liquid xenon and were performed in a specially designed cryostat cell. A complete description of the system can be found elsewhere.[12] For each temperature investigated, 100 interferograms were recorded at 1.0 cm^{-1} resolution, averaged, and transformed with a boxcar truncation function.

The Raman spectra (3300−10 cm^{-1}, Figure 4) were recorded on a Cary model 82 spectrophotometer using a Spectra-Physics model 171 argon ion laser operating on the 5145 Å line. The laser power varied from 0.2 to 3 W depending on the phase of the sample under investigation. The spectrum of gaseous vinyl silyl fluoride was recorded by using a standard multipass accessory. The spectrum of the liquid was obtained with the sample sealed in a glass capillary tube. The spectrum of the solid was obtained by condensing the sample onto a blackened brass plate maintained at about −196 °C by boiling liquid nitrogen, and the sample was repeatedly annealed until no further changes in the spectrum were observed. All measured frequen-

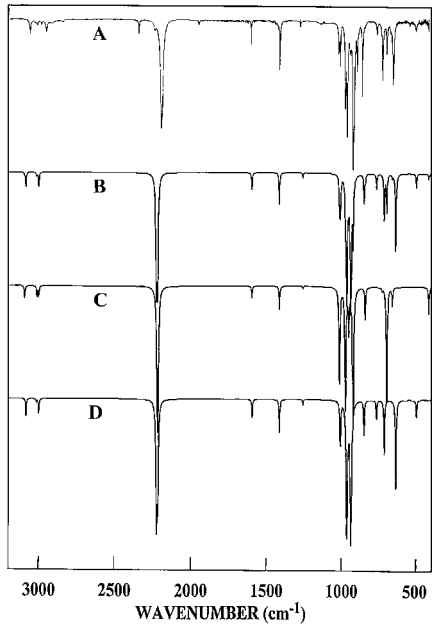

Figure 3. Predicted and observed Infrared spectra of vinyl silyl fluoride: (A) observed spectrum the sample dissolved in liquid krypton at −125 °C; (B) predicted spectrum of the mixture of gauche and cis conformers at −125 °C with $\Delta H = 76$ cm^{-1}; (C) predicted spectrum of pure cis conformer; and (D) predicted spectrum of pure gauche conformer.

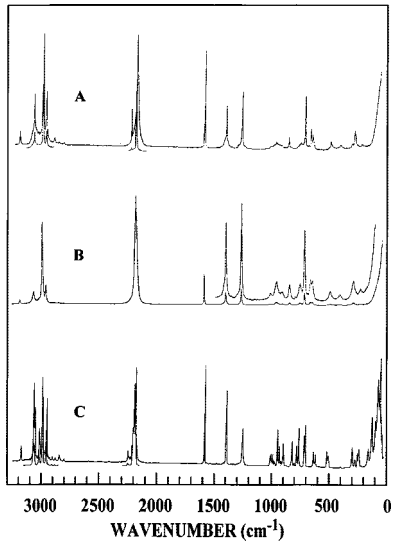

Figure 4. Raman spectra of vinyl silyl fluoride: (A) gas, (B) liquid, and (C) solid.

cies are expected to be accurate to ±2 cm^{-1}. All of the pronounced bands in the infrared and Raman spectra are listed in Table 1S in the Supporting Information and the observed fundamental modes of the gauche and cis conformers are listed in Tables 1 and 2, respectively.

Ab initio Calculations

The LCAO-MO-SCF calculations were performed with the Gaussian-03 program[13] using Gaussian-type basis functions. The energy minima with respect to nuclear coordinates were obtained by the simultaneous relaxation of all of the geometric parameters using the gradient method of Pulay.[14] Basis sets up to 6−311+G(2df,2pd) were employed at the level of restricted Hartree−Fock, Møller−Plesset perturbation theory[5] to the second order with valence and core electron correlation (MP2(full)), as well as hybrid density functional theory by the B3LYP method[9,10] to predict the conformational stability of the gauche and cis forms of vinyl silyl fluoride (Table 2S).

Ab initio MP2/6−31G(d) calculations were utilized to obtain force constants for both conformers and the resulting wavenumbers were used to aid the vibrational assignment. In order to obtain the approximate descriptions of the normal modes, *ab initio* force fields of Cartesian coordinates were transformed into force fields in internal coordinates. The corresponding transformation matrices, **B**, were generated[12] by using the Cartesian coordinates obtained from the optimized geometries. The complete set of internal coordinates, listed in Table 3, was used to form the symmetry coordinates listed in Table 3S of the Supporting Information. The resulting force fields in internal coordinates for the gauche and cis conformers are listed in Table 4S of the Supporting Information. The diagonal elements of the force field in the internal coordinates were then modified with scaling factors of 0.88 for CH and SiH stretches, 0.90 for the C=C, C−Si, and Si−F stretches and CH and SiH bends, and 1.0 for heavy atom bends and asymmetric torsion, along with geometric average of the off-diagonal elements to obtain the "fixed scaled" force fields and scaled vibrational wavenumbers, along with the potential energy distributions (P.E.D.s) listed in Tables 1 and 2, for the gauche and cis conformers, respectively.

Infrared and Raman spectra were simulated using the infrared intensities and Raman scattering activities determined from the MP2/6−31G(d) frequency calculations.[15,16] The infrared intensities were calculated with $(N\pi)/(3c^2)$ $[(\partial\mu_x/\partial Q_i)^2 + (\partial\mu_y/\partial Q_i)^2 + (\partial\mu_z/\partial Q_i)^2]$. The predicted infrared spectra of the pure cis and the gauche conformers are shown in spectra C and D in Figure 3, respectively. The predicted spectrum of a mixture of the two conformers, with a ΔH of 76 cm^{-1} with the gauche conformer more stable, is shown in Figure 3B. The ΔH value is taken from the temperature-dependent measurements in liquid krypton solution performed in this study (see the Conformational Stability section). The predicted infrared spectrum was very useful for identifying bands because of the two conformers in the infrared spectrum of the sample dissolved in liquid krypton (Figure 3A).

Similarly, the Raman scattering cross section, $\partial\sigma_j/\partial\Omega$, which is proportional to the Raman activity, can be calculated from the scattering activities and the predicted frequencies for each normal mode.[17,18] The simulated Raman spectra for the gauche and cis conformers and the mixture at 25 °C with the gauche conformer more stable by 76 cm^{-1} are shown in spectra D, C, and B in Figure 5, respectively. These spectra, when compared to the experimental Raman spectrum of the liquid (Figure 5A) recorded at room temperature, provide support for the assignment of the observed fundamentals of the two conformers.

Vibrational Assignment

In order to determine the conformational stability, it is necessary to confidently assign fundamental modes to each conformer. The proposed assignments are based on the available experimental data as well as the predicted scaled vibrational frequencies, infrared intensities, Raman activities, Raman depolarization ratios, and gas-phase infrared band contours which were compared to the corresponding experimental data. Additionally, the assignments were assisted by comparison to the previously reported vibrational assignments of the two conformers of vinyl silyl chloride.[7] The spectra of these two compounds

TABLE 1: Observed and Calculated Frequencies (cm^{-1}) for gauche Vinyl Silyl Fluoride

							IR				Raman						
vib. no.	approx. description	MP2/ 6−31G(d)	fixed scaled[a]	IR int.[b]	Raman act.[c]	dp ratio[c]	gas	liq. Kr	liq. Xe	solid	gas	liquid	Solid	P.E.D.[d]	A*	B*	C*
ν_1	CH_2 antisym. stretch	3285	3081	11.7	63.2	0.63	3068	3064	3060	3060	3070	3067	3069	$99S_1$	39	25	36
ν_2	CH stretch	3213	3014	2.2	129.3	0.26	2997	2991	2987	2992	2998	2990	2993	$89S_2$	33	26	41
ν_3	CH_2 sym. stretch	3196	2998	9.6	57.1	0.18	2967	2958	2955	2953	2967	2960	2954	$90S_3$	59	0	41
ν_4	SiH_2 antisym. stretch	2343	2198	198.1	54.8	0.68	2191	2187	2184	2194	2192	2188	2198	$100S_4$	8	2	90
ν_5	SiH_2 sym. stretch	2335	2190	117.1	129.0	0.07	2186	2187	2184	2183	2192	2188	2186	$100S_5$	13	84	3
ν_6	C═C stretch	1678	1592	12.1	3.6	0.20	1599	1596	1594	1593	1601	1596	1593	$60S_6$, $34S_7$	90	5	5
ν_7	CH_2 deformation	1488	1411	23.1	12.5	0.38	1410	1407	1405	1406	1411	1408	1406	$66S_7$, $26S_6$	72	0	28
ν_8	CH in-plane bend	1323	1257	3.8	7.6	0.40	1272	1270	1269	1274	1274	1273	1266	$59S_8$, $26S_{10}$	92	2	6
ν_9	CH_2 twist	1061	1007	11.9	2.3	0.74	1013	1014	1013	1014	1013	1018	1012	$34S_9$, $27S_{10}$, $15S_{18}$, $13S_8$	10	2	88
ν_{10}	CH_2 wag	1057	1002	31.3	2.1	0.74	1004	1004	1003	996			997	$32S_{10}$, $30S_9$, $16S_8$, $14S_{18}$	29	70	1
ν_{11}	SiH_2 deformation	1015	963	228.7	11.8	0.64	963	958	956	950	963	966	956	$47S_{11}$, $23S_{13}$, $18S_{12}$	31	66	3
ν_{12}	CH_2 rock	1001	950	7.0	3.1	0.68		938	935	944			940	$73S_{12}$, $18S_{11}$	11	43	46
ν_{13}	SiF stretch	987	936	325.1	10.4	0.75	923	916	913	900	923	914	907	$58S_{13}$, $29S_{11}$	91	6	3
ν_{14}	SiH_2 wag	892	846	24.5	5.7	0.57	861	856	853	830	861	850	831	$82S_{14}$, $15S_{13}$	22	78	0
ν_{15}	SiH_2 twist	802	762	12.6	12.2	0.75	755	756	755	773	755	755	771	$86S_{15}$	24	7	69
ν_{16}	SiC stretch	747	712	42.4	5.3	0.23	717	717	716	715	719	718	716	$53S_{16}$, $24S_{17}$	7	20	73
ν_{17}	SiH_2 rock	665	632	80.8	3.7	0.35	651	646	645	654	652	647	644	$53S_{17}$, $21S_{16}$	17	24	59
ν_{18}	CH out-of-plane bend	511	488	11.9	7.9	0.69	492	490	489	511	491	491	508	$42S_{18}$, $22S_9$, $12S_{20}$	0	95	5
ν_{19}	SiCC bend	291	285	0.2	2.5	0.57	295			303	285	287	304	$74S_{19}$	11	3	86
ν_{20}	CSiF bend	230	227	6.3	4.8	0.75	225			247	220	224	244	$72S_{20}$, $12S_{19}$	54	37	9
ν_{21}	asymmetric torsion	95	95	0.4	5.6	0.75	87			86			90	$88S_{21}$	28	12	60

[a] Scaling factors of 0.88 for CH and SiH stretches, 0.90 for the C═C, C−Si, and Si−F stretches, as well as CH and SiH bends, and 1.0 for heavy atom bends and asymmetric torsion. [b] Infrared intensities in km/mol from MP2/6−31G(d) calculation. [c] Raman activities in $Å^4/u$ and depolarization ratios from MP2/6−31G(d) calculation. [d] Calculated with MP2/6−31G(d) and contributions of less than 10% are omitted. * A, B, and C values in the last three column are percentage infrared band contours.

TABLE 2: Observed and Calculated Frequencies (cm^{-1}) for cis Vinyl Silyl Fluoride

								IR			Raman					
	vib no.	approx. description	MP2/ 6−31G(d)	fixed scaled[a]	IR int.[b]	Raman act.[c]	Dp ratio[c]	gas	liq. Kr	liq. Xe	gas	liquid	P.E.D.[d]	A*	B*	C*
A′	ν_1	CH_2 antisym. stretch	3295	3091	8.1	58.6	0.71	3076	3064	3060	3070	3067	$99S_1$	84	16	
A′	ν_2	CH stretch	3196	2998	7.3	37.1	0.74	2967	2958	2955	2967	2960	$62S_2$, $37S_3$	6	94	
A′	ν_3	CH_2 sym. stretch	3209	3010	6.3	154.0	0.15	2997	2991	2987	2998	2990	$62S_3$, $37S_2$	100	0	
A″	ν_4	SiH_2 antisym. stretch	2336	2192	108.1	66.5	0.75	2186	2187	2184	2192	2188	$100S_4$			100
A′	ν_5	SiH_2 sym. stretch	2335	2190	147.8	172.9	0.08	2186	2187	2184	2192	2188	$100S_5$	48	52	
A′	ν_6	C═C stretch	1679	1593	7.3	2.1	0.17	1599	1596	1594	1596	1593	$62S_6$, $31S_7$	63	37	
A′	ν_7	CH_2 deformation	1486	1410	15.3	13.5	0.43	1410	1407	1405	1411	1408	$68S_7$, $24S_6$	45	55	
A′	ν_8	CH in-plane bend	1321	1255	1.4	7.2	0.27	1252	1270	1269	1274	1273	$59S_8$, $27S_{10}$	46	54	
A″	ν_9	CH_2 twist	1060	1005	28.5	0.1	0.75	1004	1004	1003			$66S_9$, $26S_{18}$			100
A′	ν_{10}	CH_2 wag	1065	1012	96.1	4.5	0.54	1013	1014	1013	1013	1018	$41S_{10}$, $22S_8$, $18S_{13}$	20	80	
A′	ν_{11}	SiH_2 deformation	1024	972	159.8	27.3	0.75	970	969	966	973	970	$88S_{11}$	55	45	
A″	ν_{12}	CH_2 rock	1000	949	24.6	0.1	0.75	962	938	935			$92S_{12}$			100
A′	ν_{13}	SiF stretch	971	921	279.8	7.6	0.69	923	910	908			$56S_{13}$, $21S_{10}$, $15S_{14}$	88	12	
A′	ν_{14}	SiH_2 wag	884	839	22.5	6.4	0.63	860	856	853	861	850	$77S_{14}$, $21S_{13}$	25	75	
A″	ν_{15}	SiH_2 twist	761	722	0.4	9.2	0.75	729	723				$93S_{15}$			100
A′	ν_{16}	SiC stretch	692	651	12.5	8.6	0.22	667	665	660	667	664	$85S_{16}$	48	52	
A″	ν_{17}	SiH_2 rock	728	691	134.8	1.6	0.75	691	685	687			$83S_{17}$, $11S_{18}$			100
A″	ν_{18}	CH out-of-plane bend	417	396	0.1	2.8	0.58	403	403	404	405	406	$55S_{18}$, $21S_9$, $17S_{17}$			100
A′	ν_{19}	SiCC bend	421	414	18.3	1.9	0.63	432	430	429		428	$47S_{19}$, $46S_{20}$	79	21	
A′	ν_{20}	CSiF bend	177	174	2.3	0.4	0.66	173			171	172	$52S_{20}$, $46S_{19}$	82	18	
A″	ν_{21}	asymmetric torsion	112	112	0.5	6.3	0.75	102					$100S_{21}$			100

[a] Scaling factors of 0.88 for CH and SiH stretches, 0.90 for the C═C, C−Si, and Si−F stretches, as well as CH and SiH bends, and 1.0 for heavy atom bends and asymmetric torsion. [b] Infrared intensities in km/mol from MP2/6−31G(d) calculation. [c] Raman activities in $Å^4/u$ and depolarization ratios from MP2/6−31G(d) calculation. [d] Calculated with MP2/6−31G(d) and contributions of less than 10% are omitted. * A, B, and C values in the last three column are percentage infrared band contours; blank entries are symmetry forbidden.

look remarkably similar down to about 1000 cm^{-1}, with nearly the same assignments made for the fundamentals above this frequency.

The predicted gas phase infrared band contours (see Figure 1S in the Supporting Information) were particularly helpful for the vibrational assignment. Complete assignments of the gauche and cis conformers are reported in Tables 1 and 2, respectively. It is of particular interest to examine the low-frequency region where the bands are usually more indicative of the presence of conformer. The CSiF bend is predicted at 227 and 174 cm^{-1} for the gauche and cis forms, respectively. The Q-branch of an A/B hybrid band at 225 cm^{-1} in the infrared spectrum of the vapor (220 cm^{-1} in the Raman spectrum) is assigned to the gauche conformer. This assignment is consistent with the microwave results,[8] where the CSiF bending mode for the gauche conformer was estimated at 181 ± 39 cm^{-1}. The Q-branch at 173 cm^{-1} as a shoulder on the stronger A/B hybrid band (Figure 1) in the infrared spectrum (171 cm^{-1} Raman spectrum) is confidently assigned as the CSiF bend for the cis conformer. The asymmetric torsion is predicted at 95 and 112 cm^{-1} for the gauche and cis forms, respectively. We assigned the series of hot bands which begin at 102.34 cm^{-1} with subsequent sharp Q-branches falling to lower frequencies to the asymmetric torsion of the cis conformer, whereas another set of Q-branches between 86.56 and 75.82 cm^{-1} are assigned to the gauche conformer. This assignment is consistent with the

TABLE 3: Structural Parameters (Å and deg), Rotational Constants (MHz) and Dipole Moments (debye) for CH_2=$CHSiH_2X$ (X = F, Cl, CH_3)

		vinyl silyl fluoride								vinyl silyl chloride		methyl vinyl silane	
		RHF/6−31G(d)		MP2(full)/6−311+G(d,p)		MW[a]		adjusted r_0		adjusted r_0		adjusted r_0	
param	int. coord.	gauche	cis	gauche	cis	gauche	cis	gauche	cis	gauche	cis	gauche	cis
rSi_1-X_2	T	1.599	1.598	1.627	1.627	1.597	1.597	1.596(5)	1.593(5)	2.056(5)	2.052(5)	1.871(5)	1.867(5)
rC_3−Si_1	R_1	1.859	1.861	1.850	1.853	1.853	1.853	1.846(5)	1.849(5)	1.845(5)	1.851(5)	1.862(5)	1.863(5)
rC_3=C_4	R_2	1.326	1.325	1.347	1.346	1.347	1.347	1.345(5)	1.344(5)	1.344(5)	1.343(5)	1.345(5)	1.344(5)
rSi_1H_5	r_4	1.472	1.472	1.471	1.472	1.477	1.477	1.477(3)	1.478(3)	1.477(2)	1.476(2)	1.487(2)	1.487(2)
rSi_1H_6	r_5	1.471	1.472	1.472	1.472	1.477	1.477	1.478(3)	1.478(3)	1.478(2)	1.476(2)	1.487(2)	1.487(2)
rC_3H_7	r_3	1.080	1.081	1.089	1.090	1.094	1.094	1.089(2)	1.090(2)	1.089(2)	1.091(2)	1.091(2)	1.090(2)
rC_4H_8	r_1	1.077	1.077	1.087	1.087	1.097	1.097	1.087(2)	1.087(2)	1.087(2)	1.087(2)	1.087(2)	1.087(2)
rC_4H_9	r_2	1.077	1.076	1.088	1.087	1.097	1.097	1.088(2)	1.087(2)	1.087(2)	1.086(2)	1.088(2)	1.087(2)
$\angle C_3Si_1F_2$	ω	110.3	107.8	110.2	107.7	110.5*	109.6*	110.1(5)	108.1(5)	109.7(5)	109.8(5)	110.9(5)	111.3(5)
$\angle C_4$=C_3Si_1	π	122.0	122.7	121.1	122.5	119.2*	120.3*	120.8(5)	122.5(5)	121.4(5)	124.1(5)	122.5(5)	123.8(5)
$\angle H_5Si_1C_3$	θ_1	111.6	111.7	112.1	112.0	112.5	112.5	112.1(5)	111.9(5)	111.9(5)	111.3(5)	110.0(5)	109.3(5)
$\angle H_6Si_1C_3$	θ_2	109.1	111.7	108.9	112.0	112.5	112.5	108.8(5)	111.9(5)	108.8(5)	111.3(5)	107.3(5)	109.3(5)
$\angle H_7C_3Si_1$	ψ_2	119.8	119.0	120.9	119.6	128.6	127.7	120.9(5)	119.6(5)	120.2(5)	117.8(5)	119.9(5)	119.3(5)
$\angle H_8C_4$=C_3	β_1	122.4	122.2	122.1	121.8	120.6	120.6	122.1(5)	121.8(5)	121.9(5)	121.5(5)	122.1(5)	121.9(5)
$\angle H_9C_4$=C_3	β_2	122.1	121.9	121.6	121.5	120.3	120.3	121.6(5)	121.5(5)	121.5(5)	121.5(5)	121.4(5)	121.7(5)
τC_4=$C_3Si_1F_2$	τ	117.2	0.0	117.2	0.0	120.0	0.0	119.7(5)	0.0	120.4(5)	0	120.6(5)	0
$\tau H_5Si_1C_3F_2$		118.5	118.8	118.1	118.0			118.8(5)	118.4(5)	118.5(5)	118.8(5)	120.9(5)	121.1(5)
$\tau H_6Si_1C_3F_2$		−119.0	−118.8	−118.1	−118.0			−118.2(5)	−118.4(5)	−118.3(5)	−118.8(5)	−120.4(5)	−121.1(5)
$\tau H_7C_3Si_1C_4$	ξ_2	178.9	180	178.8	180	180	180	180	180	180	180	180.8	180
τH_8C_4=C_3Si_1	μ	178.8	180	178.8	180	180	180	180	180	180	180	180.5	180
τH_9C_4=C_3H_8	ξ_1	179.9	180	179.9	180	180	180	180	180	180	180	180.2	180
$\lvert\mu_a\rvert$		1.931	1.323	2.240	1.450	1.700	1.176						
$\lvert\mu_b\rvert$		0.672	1.025	0.976	1.367	0.56	0.950						
$\lvert\mu_c\rvert$		0.189		0.207		0.23	0.000						
$\lvert\mu_{tot}\rvert$		2.053	1.674	2.452	1.993	1.800	1.512						

[a] See ref 9; all parameters were assumed except for CSiF and CCSi angles (marked with asterisk), which were obtained from a fit of the rotational constants.

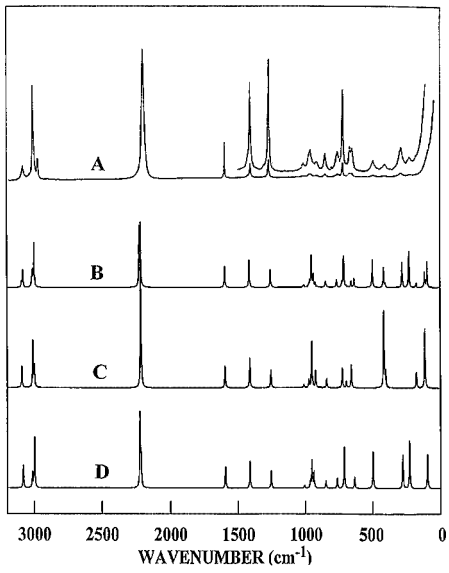

Figure 5. Predicted and observed Raman spectra of vinyl silyl fluoride: (A) observed spectrum of liquid at 25 °C; (B) predicted spectrum of the mixture of gauche and cis conformers at 25 °C with ΔH = 76 cm^{-1}; (C) predicted spectrum of pure cis conformer; and (D) predicted spectrum of pure gauche conformer.

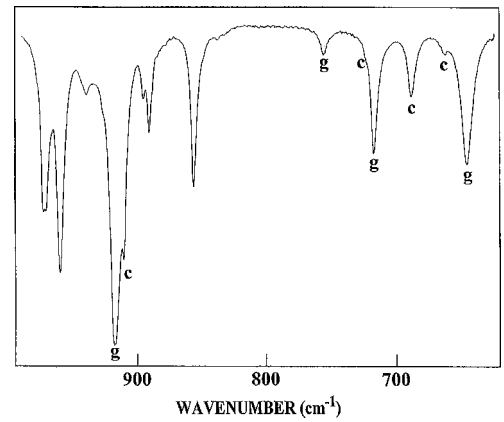

Figure 6. Infrared spectra of vinyl silyl fluoride dissolved in liquid krypton at −140 °C, some of the conformer bands are indicated by "c" for cis and "g" for gauche.

estimated torsional frequency of 74 ± 18 cm^{-1} for the gauche conformer from the microwave investigation.

Conformational Stability

To determine the enthalpy difference between the two conformers, variable-temperature studies in liquid krypton and xenon were carried out. Because only small interactions are expected to occur between the dissolved molecules and the surrounding noble gas atoms,[19−22] the "pseudo gas phase" spectrum shows only small frequency shifts compared with the spectrum of the gas. A significant advantage of this type of cryogenic spectroscopic study is that the conformer bands are better resolved in comparison with those in the spectrum of the gas. This is particularly important because most of the conformer bands for this molecule are expected to be observed within a few wavenumbers of each other. The different conformer bands that can be clearly identified in the spectral region between 1000 and 600 cm^{-1} of the krypton solution are shown in Figure 6, and the ones indicated are due to the individual conformers.

The sample was dissolved in the liquified noble gases and the spectra were recorded at varying temperatures as indicated earlier. The spectral changes in liquid krypton of some conformer bands are shown in Figure 7. Of the several fundamental modes exhibiting conformer doublets, the 717 cm^{-1} (gauche) and 685 cm^{-1} (cis) pair was initially chosen for the conformational enthalpy determination because of their relatively even baseline, satisfactory band separations, and relatively strong band intensities. The relative intensities of this conformer pair

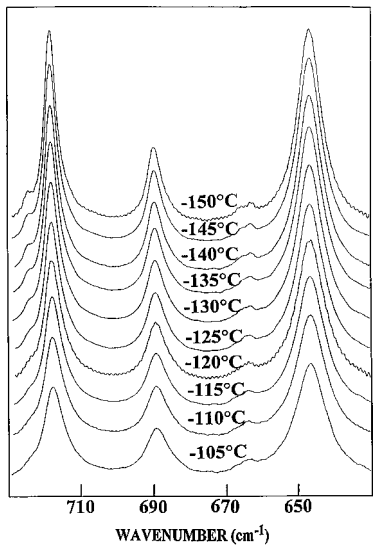

Figure 7. Temperature dependence of the 717 cm^{-1} (gauche) and the 689 cm^{-1} (cis) infrared bands of vinyl silyl fluoride dissolved in liquid krypton.

were measured as a function of temperature and their ratios were determined. Ten sets of spectral data were obtained for the pair and by application of the van't Hoff equation, $-\ln K = \Delta H/(RT) - \Delta S/R$. The enthalpy difference was determined from a plot of $-\ln K$ versus $1/T$ (see Figure 2S in the Supporting Information), where $\Delta H/R$ is the slope of the line and K is substituted with the appropriate intensity ratios, i.e., I_{cis}/I_{gauche}. It was assumed that ΔH, ΔS, and the ratio of the molar absorption coefficients $\varepsilon_{gauche}/\varepsilon_{cis}$ are not a function of temperature in the temperature range studied. The conformational enthalpy difference was determined to be 73 ± 7 cm^{-1} (0.87 ± 0.08 kJ/mol) from the krypton solution for this pair. Two other pairs of fundamentals were also utilized (916 gauche/910 cis and 646 gauche/685 cis), from which two additional ΔH values were obtained. The three individual values are listed in Table 4 and the statistical average was obtained by treating all the data as a single set, which gave a value of 76 ± 7 cm^{-1} (0.91 ± 0.08 kJ/mol). Another ΔH value was obtained from a xenon solution with the 717/685 cm^{-1} pair where these two bands were still sufficiently separated but the shoulders of the other two pairs were too close to the other bands to use to obtain ΔH values. The determined ΔH value, from the xenon solution, of 69 ± 7 cm^{-1} had a similar value to that obtained from the krypton solution.

We also carried out a variable-temperature Raman study of the gas for vinyl silyl fluoride in order to evaluate the probable difference from the values of the rare gas in solutions. The two lines at 667 and 719 cm^{-1} in the Raman spectrum of the gas are the only well resolved conformer doublet where the relative intensities could be measured as a function of temperature in the Raman spectrum. Six sets of spectral data were obtained at temperatures varying from 24 to 85 °C (Table 4). At each temperature the spectrum was recorded four times and the average area ratio was used in the calculations. From the slope of the plot, ΔH was determined to be 133 ± 27 cm^{-1}. Several attempts were made to obtain the ΔH value of the liquid over a range of temperatures from 24 to −130°, but without success. We found that the results were inconclusive probably due to small immeasurable changes in the line intensities, as a result of a very small ΔH value in the liquid, as well as difficulty in maintaining the temperature uniformly over the Raman cell holding the liquid.

Torsional Potential Function

The far-infrared spectrum of gaseous vinyl silyl fluoride (Figure 2) shows two sets of transitions below 120 cm^{-1}. The asymmetric torsions are predicted by ab initio MP2(full)/6−31G(d) calculations to be at 94 and 112 cm^{-1} for the gauche and cis forms, respectively. Therefore, we assigned the series which begin at 102.34 cm^{-1} with subsequent sharp Q-branches falling to lower frequencies to the asymmetric torsion of the cis conformer, whereas another set of Q-branches between 86.56 and 75.82 cm^{-1} are assigned to that of the gauche conformer. This assignment is consistent with the estimated torsional frequency of 74 ± 18 cm^{-1} for the gauche conformer from the microwave investigation.[8]

By using the adjusted r_0 structural parameters (Table 3, described in the Structural Parameters section) we calculated the internal rotational constant, F, as a function of the C═CSiF dihedral angle ϕ, with structural relaxation according to the following equations

$$F(\varphi) = F_0 + \sum_{i=1}^{n} F_i \cos i\varphi \; V(\varphi) = \frac{1}{2}\sum_{i=1}^{n} V_i(1 - \cos i\varphi) \quad (1)$$

The relaxation of the structural parameters, $B(\phi)$, during the internal rotation can be incorporated into the above equation by assuming them to be small periodic functions of the torsional angle, ϕ, of the general type

$$B(\varphi) = a + b\cos\varphi + c\sin\varphi \quad (2)$$

where a, b, and c are constants. The torsional potential function used to fit the observed frequencies is also assumed to be a periodic function in ϕ.

For the initial calculations, the ground-state and the first-excited-state torsional transitions of each conformer along with the experimentally determined conformational enthalpy difference of 76 cm^{-1} were used. It was found from these initial calculations that there are strong correlations between the V_1 and V_2 potential terms. Therefore, it was necessary to find a suitable combination of these two coefficients that would give a minimum dispersion for all the potential coefficient terms, the first four observed torsional transitions, as well as a reasonable value for the dihedral angle. Initially, the dihedral angle was restricted to values between 117.2 and 120° that were taken from the ab initio MP2(full)/6−311+G(d,p) level of calculation and the microwave data, respectively. In the final calculations, additional transitions were added and the dihedral angle was restricted to a smaller range of values and a higher weight was given to this parameter. Additionally, it was necessary to use the V_4 and V_6 terms in the calculations to obtain the best fit between the experimental and the calculated torsional values, whereas using the V_5 term increased the dispersion without improving the fit so it was set to zero. The results of these calculations are listed in Table 5 and they are compared to the potential coefficients obtained from ab initio MP2(full)/6−311+G(d,p) calculations. The resulting potential function governing conformational interchange is shown in Figure 8.

r_0 Structural Parameters

In the previous microwave study,[8] all structural parameters were assumed for both conformers except for the two skeletal angles, ∠SiCC and ∠CSiF, which were varied to fit the rotational constants. For the cis conformer, the CH_2═$CHSiH_2F$ and CH_2═$CHSiD_2F$ isotopomers provided six rotational constants to give the resulting fit of the SiCC (120.3°) and CSiF (109.6°) angles (Table 3). For the gauche conformer, a total of

TABLE 4: Temperature and Intensity Ratios (I_{gauche}/I_{cis}) of the Conformational Bands of Vinyl Silyl Fluoride from the Infrared Spectra of the Liquid Krypton, Liquid Xenon Solution Phases, and Raman Spectrum of the Gas

	T (°C)	$1/T$ ($\times 10^{-3}$ K^{-1})	I_{916}/I_{910}	I_{717}/I_{685}	I_{719}/I_{667}	I_{646}/I_{685}
liquid xenon	−60.0	4.692		1.597		
	−65.0	4.804		1.604		
	−70.0	4.922		1.636		
	−75.0	5.047		1.668		
	−80.0	5.177		1.684		
	−85.0	5.315		1.693		
	−90.0	4.460		1.728		
	−95.0	5.613		1.747		
	−100.0	5.775		1.775		
ΔH				69 ± 7 cm^{-1}		
liquid krypton	−105.0	5.950	7.433	2.030		3.285
	−110.0	6.129	7.186	2.122		3.262
	−115.0	6.323	7.430	2.182		3.428
	−120.0	6.529	7.480	2.197		3.429
	−125.0	6.750	7.601	2.245		3.493
	−130.0	6.986	7.746	2.326		3.701
	−135.0	7.238	7.723	2.388		3.893
	−140.0	7.510	8.481	2.310		3.628
	−145.0	7.803	8.144	2.543		4.249
	−150.0	8.120		2.624		4.518
$\Delta H^{a,b}$			50 ± 10 cm^{-1}	73 ± 7 cm^{-1}		97 ± 13 cm^{-1}
gas	85	2.79			0.384	
	68	2.93			0.399	
	53	3.07			0.411	
	44	3.15			0.414	
	35	3.25			0.423	
	24	3.37			0.429	
ΔH					133 ± 27 cm^{-1}	

[a] Average value: $\Delta H = 76 \pm 7$ cm^{-1} (0.91 ± 0.08 kJ/mol) with the gauche conformer more stable. [b] Value obtained by utilizing all data as a single set.

TABLE 5: Observed and Calculated[a] Asymmetric Torsional Transitions (cm^{-1}), Potential Energy Parameters (cm^{-1}), and Barriers to Internal Rotation for Vinyl Silyl Fluoride

conformer	transition	obsd	calcd[a]	Δ (calcd − obsd)
gauche	∓1 ← ± Z0	86.56	86.08	−0.48
	∓2 ← ± Z1	84.58	84.43	−0.15
	∓3 ← ± Z2	81.42	82.15	0.73
	∓4 ← ± Z3	78.63	79.17	0.54
	∓5 ← ± Z4	75.82	75.28	−0.54
cis	1 ← 0	102.34	102.79	0.45
	2 ← 1	98.31	98.48	0.17
	3 ← 2	93.91	93.19	−0.72

parameter	experimental	MP2(full)/6−311+G(d,p)
V_1	−80 ± 11	−2
V_2	−42 ± 15	−197
V_3	622 ± 5	517
V_4	34 ± 5	−22
V_6	−31 ± 2	−4
gauche-to-cis barrier	664	527
gauche-to-gauche barrier	608	683
cis-to-gauche barrier	598	354
gauche C═CSiF dihedral angle (deg)	119.7	117.2
ΔH (ΔE)	76	175

[a] Calculated using the potential constants and internal rotational constant series $F_0 = 1.9090635$, $F_1 = 0.1233579$, $F_2 = 0.0884255$, $F_3 = 0.0159960$, $F_4 = 0.0062688$, $F_5 = 0.0013674$, $F_6 = 0.0004759$ cm^{-1}, $F_7 = 0.0001215$ cm^{-1}, and $F_8 = 0.0000362$ cm^{-1}.

eight rotational constants were obtained from the SiH_2, Si-d_2, and $^{29}SiH_2$ (B and C) isotopomers, which gave the corresponding SiCC (119.2°) and CSiF (110.5°) angle with the skeletal FSiCC dihedral angle fixed at 120° (Table 3).

Because all bond distances and hydrogen angles were fixed at assumed values and kept the same for both conformers and the gauche skeletal angle was fixed at 120°, the resulting structural parameters reported from the microwave study involve relatively large uncertainties.[8] Thus, we initiated a reinvestigation of the r_0 structural parameters of vinyl silyl fluoride. We have found that one can obtain good structural parameters by systematically adjusting the structural parameters from ab initio calculations to fit the rotational constants obtained from the microwave spectroscopic data (computer program "A&M" (ab initio and microwave),[1] developed in our laboratory). To reduce the number of independent variables, we separated the structural parameters into sets according to their types, i.e., bond lengths in the same set keep their relative ratio, and bond angles and torsional angles in the same set keep their differences in degrees. This assumption is based on the fact that errors from ab initio calculations are primarily systematic.

Recently, we have shown[23] for more than 50 carbon−hydrogen distances that the r_e distances predicted at MP2(full)/6−311+G(d,p) level of calculation match the r_0 distances determined from the "isolated" CH stretching frequencies[24] to within ±0.002 Å. Considering this level of accuracy in the CH predictions as well as the small mass of the hydrogen atom, the effect on the rotational constants from the errors of the MP2(full)/6−311+G(d,p) predicted CH parameters are orders of magnitude smaller than those from the skeletal structure. Thus, it is possible to reduce the number of independent structural parameters significantly by fixing the CH parameters at MP2(full)/6−311+G(d,p) optimized values.

With the six reported[8] rotational constants as well as a set of relative weights of the different types of structural parameters (a 1% error of rotational constant is equivalent to a 5% shift of

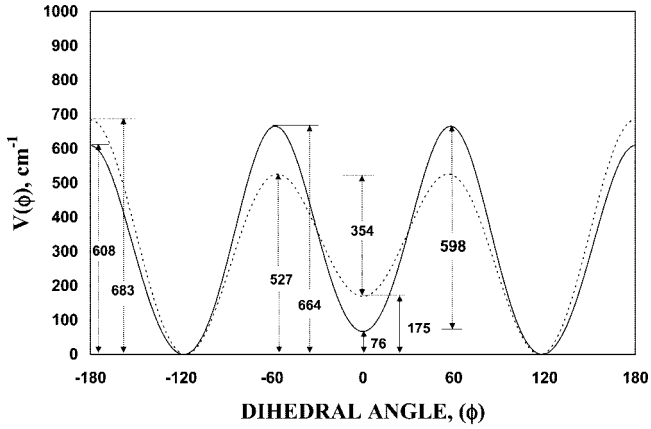

Figure 8. Potential function governing the asymmetric torsion of vinyl silyl fluoride obtained from MP2(full)/6−311+G(d,p) calculations (dashed line), from the fit of the asymmetric torsional transitions with conformational enthalpy difference of 76 cm^{-1} (bold solid line).

a bond length, or a 10° shift of bond angle, or a 50° shift of torsional angle) implemented in the A&M program,[1] the "adjusted" r_0 structural parameters of the cis conformer of vinyl silyl fluoride can be uniquely obtained.

It has been found that ab initio MP2 calculations systematically give poor predictions of the Si−F distance by overestimating the value by about 0.02 to 0.03 Å.[25] However, the Si−F distance predicted at Hartree−Fock level are significantly better, usually with errors of less than 0.005 Å of the experimentally determined r_0 distances.[26] Thus, we utilized the Si−F bond distances optimized at the RHF/6−31G(d) level in the initial input of the A&M program. In addition, it has been shown that SiH distances can be obtained from the frequencies of the isolated SiH stretching frequencies.[27] Therefore, we have obtained values of 1.477 and 1.478 Å for the r_4 and r_5 distances (Table 3) which are 0.006 Å longer than values for the corresponding distances from the ab initio predicted parameters. This value of 0.006 Å is the same difference found for many SiH parameters in other organosilanes.[28,29] With the exception of the changes to the two parameters described, the rest of the equilibrium structural parameters optimized at the MP2(full)/6−311+G(d,p) level are taken as the initial input of the A&M program. The resulting "adjusted" r_0 structural parameters for the cis conformer are listed in Table 3, along with the previously proposed structure from the microwave study[8] and the ab initio predicted values. The same treatment was applied to the determination of the r_0 structure of the gauche conformer for which a total of eight rotational constants from three isotopomers were available.[8] In addition, the vinyl moiety was kept planar to further reduce the number of independent variables. The resulting "adjusted" r_0 structural parameters for the gauche conformer are also listed in Table 3.

There are only four determined structural parameters thaat have significantly different values between the two conformers and these are the SiF and CSi distances which differ by 0.003 Å and the ∠CSiF and ∠CCSi which differ by about 2°. We believe these experimental reported parameters should have relatively small uncertainties of 0.005 Å for the heavy atom distances, 0.002 and 0.003 Å for the CH and SiH distances, respectively, and 0.5° for the angles. The adjusted r_0 values are probably as accurate as could be determined from an electron diffraction study or from r_s parameters obtained from additional microwave studies by isotopic substitution of all of the atoms.

To compare the structural parameters of the series of monosubstituted vinyl silane molecules, $CH_2{=}CHSiH_2X$, we carried out the process of obtaining the "adjusted" r_0 structural parameters for vinyl silyl chloride ($CH_2{=}CHSiH_2Cl$) and methyl vinyl silane ($CH_2{=}CHSiH_2CH_3$) from the previously reported[30,31] microwave rotational constants. The procedure was the same as described above except the initial input of the Si−Cl and the Si−C(H_3) distances in the A&M program were kept as MP2(full)/6−311+G(d,p) optimized values. The fit to the rotational constant of the fluoride, chloride and methyl substituted to the vinyl moiety is given in Tables 5S−7S in the Supporting Information.

In Table 3, the previously reported[32,33] adjusted r_0 parameters are listed for methyl vinyl silane as well as those for vinyl silyl chloride. Except for the parameters associated with the halogen atoms, the remaining parameters differ by very small amounts, such as 0.001 Å for the distance and the angles by 0.2°. However, for the methyl compound, there is a large increase of 0.016 Å for the Si to vinyl carbon distance as well a significant increase of 0.006 Å in the SiH distance for the gauche conformer,whereas for the cis conformers, the increases are a little smaller at 0.014 and 0.005 Å, respectively. These differences are expected from the large electronegativities of the halogen atoms. Also, a comparison with the structural parameters of vinyl silane[34] shows the Si−C distance in this molecule is about halfway between the corresponding distance for this parameter of the methyl and halogen substituted silicon atom. In general, the remaining parameters are remarkably similar.

Discussion

The P.E.D.s indicated relatively small amount of mixing for the fundamentals of the cis conformer with only ν_{10} and ν_{13} of the A′ species and ν_{18} (A″) which have significant contribution from three symmetry coordinates. As expected, there is considerably more mixing of the modes for the gauche conformer with C_1 symmetry where ν_9 and ν_{10} (CH_2 motions) have major contributions form four symmetry coordinates and two other with three significant contributions. Nevertheless, all of the other vibrations have more than 50% contributions from the motions indicated, as is approximately described in Table 1.

By using scaling factors of 0.88 for CH and SiH stretches; 0.90 for the C=C, C−Si, and Si−F stretches as well as CH and SiH bends; and 1.0 for heavy atom bends and asymmetric torsion, the average frequency deviation of the fixed scaled fundamentals at MP2(full)/6−31G(d) level of calculation is only 9.4 and 9.9 cm^{-1}, representing a relative error of 0.7 and 0.8%, for the gauche and cis forms, respectively. Therefore, the frequency predictions from the relatively low level MP2(full)/6−31G(d) calculations are quite accurate for this type of molecule and they facilitate the vibrational assignment. These results show that the two nonunity scaling factors are sufficient to adequately predict the frequency for the observed fundamentals for this type of molecule.

With all levels of calculation utilized in this study, the gauche conformer is predicted to be the more stable form (see Table 2S in the Supporting Information). The energy difference is predicted between 98 and 175 cm^{-1} (1.17 to 2.09 kJ/mol) with an average value of 132 ± 29 cm^{-1} (1.58 ± 0.35 kJ/mol) from the MP2 calculations with the six largest basis sets and 107 ± 27 cm^{-1} (1.28 ± 0.23 kJ/mol) from the similar prediction from the B3LYP calculations. The size of the basis set rather than the method of electron correlation seems to be the dominating factor for the predicted conformational energy difference, i.e., the 6−31G(d) basis set predicts the largest conformational energy difference whereas the 6−311+G(2d,2p) gives the smallest for both MP2 and B3LYP methods. The experimentally

determined value of 133 ± 27 cm^{-1} (1.59 ± 0.32 kJ/mol) from the Raman temperature-dependent studies of the vapor falls within the upper half of the range of the ab initio predicted values. The values of 76 ± 7 cm^{-1} (0.91 ± 0.08 kJ/mol) from the krypton solution and 69 ± 7 cm^{-1} (0.82 ± 0.08 kJ/mol) from the xenon solution agree with the lowest ab initio prediction. Additionally, the experimental data are all within the relatively large error limits of the previously reported enthalpy difference from microwave data[8] of 210 ± 140 cm^{-1} (2.51 ± 1.68 kJ/mol), with the gauche conformer more stable.

It is interesting to compare the conformational energy difference of vinyl silyl fluoride with the corresponding value for allyl fluoride.[1] For allyl fluoride, calculation at the MP2/6−311++G(d,p) level predicts the gauche conformer to be the more stable form by 117 cm^{-1} (1.40 kJ/mol), whereas the experimental enthalpy value was determined to be 130 ± 25 cm^{-1} (1.56 ± 0.30 kJ/mol) from the vapor, and 81 ± 1 cm^{-1} (0.97 ± 0.01 kJ/mol) from a liquid argon solution but with the cis form being the more stable conformer. However, for vinyl silyl fluoride, the more stable form is the gauche conformer, with ab initio calculations from modest size basis sets predicting correctly the more stable conformer. For vinyl silyl chloride, the more stable form is the cis conformer in contrast to the gauche form for the corresponding carbon analogue. The ab initio predictions seem to better predict the conformational stabilities of the organosilicon compounds compared to the carbon compounds. The conformational enthalpy difference determined from the Raman spectrum of the gas is essentially the same as the ab initio predictions, but about 20% higher than the values from the noble gas solution. Solvent influences are expected to be relatively small for the rare gas solutions but nevertheless will lower the determined value some. Also, there may be some effect due to the distribution of heat to the Raman cell to maintain a uniform temperature as well as recording the temperature of the gas. Additionally, the measurement of a single pair of lines could be a factor. Therefore the difference between the ΔH of the gas and its value in the solutions is not considered significant.

With the ΔH and structural parameters obtained in the present study, we have calculated the potential function governing the conformational interchange (Figure 8). The determined potential parameters are listed in Table 5 and compared to those obtained from ab initio MP2/6−311+G(d,p) calculations. The experimental gauche-to-cis, gauche-to-gauche, and cis-to-gauche barriers were determined to be 664 cm^{-1} (7.94 kJ/mol), 608 cm^{-1} (7.27 kJ/mol), and 598 cm^{-1} (6.89 kJ/mol), respectively, which are consistent with the corresponding MP2/6−311+G(d,p) predicted barriers except that of the cis-to-gauche, where the predicted barrier is significantly smaller than the experimentally determined value by 244 cm^{-1}. This result is significantly different from what was obtained for the corresponding carbon compound where the predicted cis-to-gauche barrier (1103 cm^{-1}) was in excellent agreement with the experimentally determined value (1117 cm^{-1}).[1] Also, it should be noted that this near 3-fold potential for the vinyl silyl fluoride[7] molecule is significantly different from the corresponding potential parameter of vinyl silyl chloride where the gauche-to-gauche barrier was one-third smaller than the other two barriers. This difference can be rationalized on the basis of the steric affect of the relative size of the chloride atom to the fluoride atom. These results indicate that the ab initio calculations for the monosubstituted vinyl silyl compounds provide reasonable predicted conformational stabilities between the conformers and do not suffer the problems which were encountered with the prediction from similar calculations for the corresponding carbon analogues.

Acknowledgment. J.R.D. acknowledges the University of Missouri−Kansas City for a Faculty Research Grant for partial financial support of this research.

Supporting Information Available: Table 1S, observed infrared and Raman frequencies (cm^{-1}) and vibrational assignment for vinyl silyl fluoride; Table 2S, calculated energies and energy differences for the gauche and cis conformers of vinyl silyl fluoride; Table 3S, symmetry coordinates for vinyl silyl fluoride; Table 4S, fixed scaled ab initio MP2(full)/6−31G(d) force constants of the gauche and cis conformers of vinyl silyl fluoride; Table 5S, comparison of rotational constants (MHz) obtained from modified ab initio MP2(full)/6−311+G(d,p) predictions, microwave spectra, and the adjusted structural parameters for vinyl silyl fluoride; Table 6S, comparison of rotational constants (MHz) obtained from modified ab initio MP2(full)/6−311+G(d,p) predictions, microwave spectra, and the adjusted structural parameters for vinyl silyl chloride; Table 7S, comparison of rotational constants (MHz) obtained from modified ab initio MP2(full)/6−311+G(d,p) predictions, microwave spectra, and the adjusted structural parameters for methyl vinyl silane; Figure 1S, predicted A-, B-, C-type gas phase infrared band envelopes for the gauche and cis conformer of vinyl silyl fluoride; Figure 2S, van't Hoff plot of the 916 cm^{-1} (gauche)/910 cm^{-1} (cis), 646 cm^{-1} (gauche)/685 cm^{-1} (cis) and the 717 cm^{-1} (gauche)/685 cm^{-1} (cis) infrared bands of vinyl silyl fluoride dissolved in liquid noble gas (PDF). This material is available free of charge via the Internet at http://pubs.acs.org.

References and Notes

(1) Van der Veken, B. J.; Herrebout, W. A.; Durig, D. T.; Zhao, W.; Durig, J. R. *J. Phys. Chem. A* **1999**, *103*, 1976.
(2) Durig, J. R.; Durig, D. T.; Van der Veken, B. J.; Herrebout, W. A. *J. Phys. Chem. A* **1999**, *103*, 6142.
(3) Durig, J. R.; Tang, Q.; Little, T. S. *J. Mol. Struct.* **1992**, *269*, 257.
(4) Durig, J. R.; Tang, Q.; Little, T. S. *J. Raman Spectrosc.* **1992**, *23*, 653.
(5) Møller, C.; Plesset, M. S. *Phys. Rev.* **1934**, *46*, 618.
(6) Galabov, B.; Kenny, J. P.; Shaefer, H. F., III; Durig, J. R. *J. Phys. Chem. A* **2002**, *106*, 3625.
(7) Durig, J. R.; Nashed, Y. E.; Qtaitat, M. A.; Guirgis, G. A. *J. Mol. Struct.* **2000**, *525*, 191.
(8) Imachi, M. *J. Sci. Hiroshima Univ., Ser. A* **1978**, *42*, 31.
(9) Becke, A. D. *J. Chem. Phys.* **1993**, *98*, 5648.
(10) Lee, C.; Yang, W.; Parr, R. G. *Phys. Rev. B* **1988**, *37*, 785.
(11) Hollandsworth, R. P.; Ingle, W. M.; Ring, M. A. *Inorg. Chem.* **1967**, *6*, 844.
(12) Guirgis, G. A.; Zhu, X.; Yu, Z.; Durig, J. R. *J. Phys. Chem. A* **2000**, *104*, 4383.
(13) Frisch, M. J. Trucks, G. W. Schlegel, G. W. Scuseria, G. E. Robb, M. A. Cheeseman, J. R. Montgomery, Jr., J. A. Vreven, T. Kudin, K. N. Burant, J. C. Millam, J. M. Iyengar, S. S. Tomasi, J. Barone, V. Mennucci, B. Cossi, M. Scalmani, G. Rega, N. Petersson, G. A. Nakatsuji, H. Hada, M. Ehara, M. Toyota, K. Fukuda, R. Hasegawa, J. Ishida, M. Nakajima, T. Honda, Y. Kitao, O. Nakai, H. Klene, M. Li, X. Knox, J. E. Hratchian, H. P. Cross, J. B. Bakken, V. Adamo, C. Jaramillo, J. Gomperts, R. Stratmann, R. E. Yazyev, O. Austin, A. J. Cammi, R. Pomelli, C. Ochterski, J. W. Ayala, P. Y. Morokuma, K. Voth, G. A. Salvador, P. Dannenberg, J. J. Zakrzewski, V. G. Dapprich, S. Daniels, A. D. Strain, M. C. Farkas, O. Malick, D. K. Rabuck, A. D. Raghavachari, K. Foresman, J. B. Ortiz, J. V. Cui, Q. Baboul, A. G. Clifford, S. Cioslowski, J. Stefanov, B. B. Liu, G. Liashenko, A. Piskorz, P. Komaromi, I. Martin, R. L. Fox, D. J. Keith, T. Al-Laham, A. Peng, C. Y. Nanayakkara, A. Challacombe, M. Gill, P. M. W. Johnson, B. Chen, W. Wong, M. W. Gonzalez, C. and Pople, J. A. *Gaussian 03, Revision D.01*; Gaussian, Inc.: Wallingford CT, (2004.
(14) Pulay, P. *Mol. Phys.* **1969**, *179*, 197.
(15) Frisch, M. J.; Yamaguchi, Y.; Gaw, J. F.; Schaefer, H. F., III; Binkley, J. S. *J. Chem. Phys.* **1986**, *84*, 531.
(16) Amos, R. D. *Chem. Phys. Lett.* **1986**, *124*, 376.

(17) Polavarapu, P. L. *J. Phys. Chem.* **1990**, *94*, 8106.
(18) Chantry, G. W. In *The Raman Effect*; Anderson, A., Ed.; Marcel Dekker: New York, 1971; Vol. 1, Chapter 2.
(19) Bulanin, M. O. *J. Mol. Struct.* **1995**, *347*, 73.
(20) Bulanin, M. O. *J. Mol. Struct.* **1973**, *19*, 59.
(21) Van der Veken, B. J.; DeMunck, F. R. *J. Chem. Phys.* **1992**, *97*, 3060.
(22) Herrebout, W. A.; Van der Veken, B. J.; Wang, A.; Durig, J. R. *J. Phys. Chem.* **1995**, *99*, 578.
(23) Durig, J. R.; Ng, K. W.; Zheng, C.; Shen, S. *Struct. Chem.* **2004**, *15*, 149.
(24) McKean, D. C.; Torto, I. *J. Mol. Struct.* **1982**, *81*, 51.
(25) Durig, J. R.; Pan, C.; Klaeboe, P.; Aleksa, V.; Guirgis, G. A. *Spectrochim. Acta* **2003**, *59A*, 2151.
(26) Pan, C.; Zhen, P.; Guirgis, G. A.; Durig, J. R. *J. Mol. Struct.* **2006**, *800*, 106.
(27) Duncan, J. L.; Harvie, J. L.; McKean, D. C.; Cradock, S. *J. Mol. Struct.* **1986**, *145*, 225.
(28) Mohamed, T. A.; Gurigis, G. A.; Nashed, Y. E.; Durig, J. R. *Struct. Chem.* **1998**, *9*, 255.
(29) Mohamed, T. A.; Gurigis, G. A.; Nashed, Y. E.; Durig, J. R. *Struct. Chem.* **1999**, *10*, 333.
(30) Imachi, M. *J. Sci. Hiroshima Univ., Ser. A* **1978**, *42*, 43.
(31) Imachi, M.; Nagayama, A.; Nakagawa, J.; Hayashi, M. *J. Mol. Struct.* **1981**, *77*, 81.
(32) Jin, Y.; Guirgis, G. A.; Durig, J. R. *Struct. Chem.* **2000**, *11*, 229.
(33) Durig, J. R.; Nashed, Y. E.; Qtaitat, M. A.; Guirgis, G. A. *J. Mol. Struct.* **2000**, *525*, 191.
(34) Shiki, Y.; Hasegawa, A.; Hayashi, M. *J. Mol. Struct.* **1982**, *78*, 185.

JP8076547